An infrared study of the dynamics of weakly bound water in crystalline hydrates

Robert M. Corn and Herbert L. Strauss

Department of Chemistry, University of California, Berkeley, California 94720
(Received 8 December 1981; accepted 9 February 1982)

Isotopic dilution studies of water molecules in weakly bound crystalline hydrates reveal a strong dependence of the infrared spectra on temperature. The infrared stretching and bending bands of dilute HDO in $NaClO_4 \cdot H_2O$ and $LiI \cdot 3H_2O$ show multiple bands at low temperature which broaden and move together as the temperature is raised. In contrast, only single narrow bands are seen in the very similar $LiClO_4 \cdot 3H_2O$. The potential in which the waters move is calculated from a simple electrostatic model. The stretching frequencies are taken to be a function of the librational coordinate of the water and the observed frequencies are then averages over the libration. This simple prescription for calculating the observed bands is that given by Redfield theory. We conclude that the observed band collapse in $NaClO_4 \cdot H_2O$ is due primarily to the increase with temperature of the in-plane water libration. At higher temperatures, the 180° flipping motion also contributes to the collapse. For $LiI \cdot 3H_2O$, the motion is a complex one involving locally ordered domains of the water molecules in the crystal.

I. INTRODUCTION

The importance of hydrogen bonding in water can hardly be overemphasized. However, the multiplicity and complexity of the different configurations in liquid water have made determination of the various hydrogen bonding interactions difficult. It has long been recognized that crystalline hydrates provide a better defined environment for the water molecule.[1] Indeed, a very large amount of data on crystalline hydrates is available.[2,3]

The present picture of the hydrates views their structure as due to a tradeoff between the preference of the water molecules for linear hydrogen bonds and the limitations imposed by the packing of the various ions in the crystal.

The most sensitive technique for determining the amount of hydrogen bonding in these hydrates has been infrared spectroscopy.[4] Use of isotopically dilute HDO molecules in a crystal hydrate eliminates the factor group splitting which would otherwise split and broaden the infrared lines.[5] The OD stretching frequency of these "uncoupled" molecules is highly dependent upon the water's immediate environment; the frequency can be red shifted from the gas phase value of HDO by up to 300 cm^{-1}. This high sensitivity has redefined the notion of a hydrogen bond. Certain water molecules in hydrates which do not appear to be participating in any hydrogen-donor interactions according to x-ray and neutron diffraction criteria show appreciable shifts in the infrared spectra. It is these "weakly bound" water molecules in which we are interested.

Weakly bound water of hydration exhibit a number of fascinating and heretofore puzzling phenomena. In many of these crystals motion is seen on the NMR time scale, disorder is seen by x-ray and neutron diffraction studies and the infrared spectra show multiple bands at low temperature. Equally interesting is the fact that very small changes in crystal structure seem to completely change the dynamics of the water molecules.

A well-studied example of such motion is seen in $NaClO_4 \cdot H_2O$. Brink and Falk[6] observed two OD stretching bands (of HDO) at low temperatures, which broaden and collapse to form one band at room temperature. These various OD stretching bands are at about 2600 cm^{-1}, considerably lower than the gas phase OD stretch which is at 2727 cm^{-1}, but not as low as the 2500 to 2400 cm^{-1} range which is typical of hydrogen bonds in hydrates. These OD frequencies as well as the long $OH \cdots O$ distances show that the water is definitely, but only weakly, hydrogen bonded to its surroundings. X-ray and neutron diffraction studies[7] show the water in an asymmetric environment with large amplitude libration in the plane of the water for the hydrogen. Deuterium quadrupole studies show a 180° flipping motion which interchanges the hydrogen atoms at room temperature.[8] The second moments of the proton NMR spectra reveal librational motion in the plane of the water molecule.[9] The current interpretation rests on a picture of a variety of motions between fixed sites and this picture leads to inconsistencies.[9] We will show that a detailed consideration of the potential function and the appropriate quantum mechanical energy levels for the motion of the water leads to a complete and consistent explanation of the various observations.

A very similar problem is presented by the pair of hydrates $LiClO_4 \cdot 3H_2O$ and $LiI \cdot 3H_2O$. The two hydrates have almost identical crystal structures.[10,11] The $LiClO_4 \cdot 3H_2O$ shows no large amplitude motion in the neutron diffraction studies and shows only single unshifted vibrational bands down to low temperatures. On the other hand, $LiI \cdot 3H_2O$ shows widely split vibrational bands indicating a subtle but definite difference in structure.[12]

In this paper, we first present detailed infrared spectra of dilute HDO in the various crystals as a function of temperature. Next, we calculate a potential for the motion of the water molecules using a simple electrostatic model and the structural information from the x-ray and neutron diffraction results. We then find that the infrared spectra can be interpreted by calculating the average position of the water molecule in the crystal

 0021-9606/82/104834-10$02.10

as a function of temperature and taking the vibrational frequencies as a simple function of this position. Finally we are able to draw conclusions concerning the correlations in the crystal that lead to the subtle difference between $LiClO_4 \cdot 3H_2O$ and $LiI \cdot 3H_2O$.

This paper is one of a number in which we interpret the infrared spectra of moving molecules using assumptions equivalent to the Redfield theory[13] used heretofore mainly in interpreting NMR spectra. Our other work has been on the motion of methyl groups in alkanes.[14]

II. EXPERIMENTAL

Crystals of $LiClO_4 \cdot 3H_2O$, $NaClO_4 \cdot H_2O$, and $LiI \cdot 3H_2O$ were obtained either by slow evaporation of aqueous solutions or by slow cooling of supersaturated solutions. The temperature and ionic concentrations were kept within the ranges known to yield the proper hydrate.[15,16] All chemicals used were of reagent grade.

Isotopically dilute crystals were achieved by recrystallization from aqueous solutions of approximately 1–10 mol% D_2O in H_2O. The HDO concentrations in the hydrates were estimated from the infrared intensities to be less than 3 mol% in the most isotopically dilute samples.

Samples of $NaClO_4 \cdot H_2O$ and $LiClO_4 \cdot 3H_2O$ were studied as mulls in perhalocarbon grease or oil (Kel F or Fluorolube) or Nujol between CaF_2 plates. The $LiI \cdot 3H_2O$ films were protected by Kel F or Nujol and were prepared by methods analogous to those of Brink and Falk.[12]

The infrared spectra were measured on a model 8000 Nicolet Fourier transform spectrometer with the use of either a TGS or a MCT/InSb sandwich detector. The nominal resolution was 0.5 cm^{-1}. The sample plate was mounted in a model 21 SC CTI-Cryogenics cryostat and the temperature controlled with a model DTC-500SP Lake Shore Cryotonics cryogenic temperature controller. Temperature measurements were estimated to be constant to 0.1 K or better and accurate to ±1 K. The temperature of a sample could be varied between 7 and 315 K.

Linewidths and line shifts were obtained by using either direct peak picking and FWHM measurements, simplex fits to single Lorentzian curves,[17] or curve analysis peak deconvolution programs.[18] The methods employed depended upon the band shape and isolability of the particular infrared lines in question. Line shifts were calculated to better than ±0.1 cm^{-1}; linewidths were calculated to ±0.1 cm^{-1} for isolated peaks.

III. POTENTIAL CALCULATIONS

Baur[19] noted in 1964 that for weakly hydrogen bonded crystalline hydrates (such as the three examined in this paper), electrostatic forces play the dominant role in determining the equilibrium configurations for the water molecules in the ionic lattice. For a number of weakly bound hydrates, he was able to match the equilibrium configurations determined by neutron diffraction with minima in the calculated electrostatic energy for the crystal. We extend this analysis by assuming that the electrostatic energy not only gives correct equilibrium configuration, but also reproduces the correct form of the potential energy surface for the large amplitude librational motions of the water molecules. Note that the calculation gives only a relative energy scale, since the charges assumed on the atoms of the water molecule are arbitrary and the short range forces are not included explicitly.

The potential functions for the rocking libration were obtained by calculating the electrostatic energy of the crystal along the librational coordinate defined by (i) fixing the geometry of the water molecules with an HOH angle of 109.5° and an OH bond distance of 0.97 Å, (ii) assuming that the water oxygen remains fixed at its position determined from the x-ray diffraction data, and (iii) rotating the molecule in the plane defined by the neutron diffraction coordinates of the hydrogen atoms. The librational angle θ is defined by the position of one of the OH bonds and is taken so that the OH position at equilibrium as determined by the neutron diffraction data is $\theta = 35.25°$. For example, if the OH bond were to move to the position which at equilibrium is the bisector of the HOH angle, θ would be 90°.

The electrostatic energy for the crystal was calculated at various values of θ. A point charge model was assumed. The charge on the water's hydrogen atoms was varied between $+0.5e$ and $+1.0e$ (the charge on the oxygen atom was always adjusted to maintain charge neutrality on the water molecule). $+0.7e$ was chosen as the hydrogen atom charge which best modeled the spectral differences of $LiI \cdot 3H_2O$ and $LiClO_4 \cdot 3H_2O$. For the perchlorate ions, a $+3.0e$ charge was placed on the chlorine and a $-1.0e$ charge on each of the oxygen atoms. The positions of all the heavy atoms were taken from the x-ray diffraction data. The calculation used Bertaut's modification[20] of Ewald's formula[21] for an infinite point-charge lattice and was performed by a FORTRAN program written for a CDC 6400 computer. The lattice sums over reciprocal space were continued until the shape of the potential as a function of θ remained constant.

IV. RESULTS AND DISCUSSION

A. $LiClO_4 \cdot 3H_2O$

$LiClO_4 \cdot 3H_2O$ is used as a reference point for our examination of the exchange mechanisms in the other two hydrates. The low temperature spectrum of the dilute HDO (Fig. 1 and Table I) exhibits only one $O^{16}D$ stretch and the frequency of this band remains constant to within 0.1 cm^{-1} throughout the entire temperature range. The band is narrow at low temperature. Broadening sets in smoothly at temperatures above 50 K. The HOD bend also displays a single peak at low temperature (1438.1 cm^{-1}), but the frequency shifts up by 3.6 cm^{-1} from 7 to 250 K. A positive shift in frequency is also observed for the HOH bend.

The infrared spectra place the water molecule in a single symmetric site at all temperatures, a picture which is in agreement with the electrostatic energy cal-

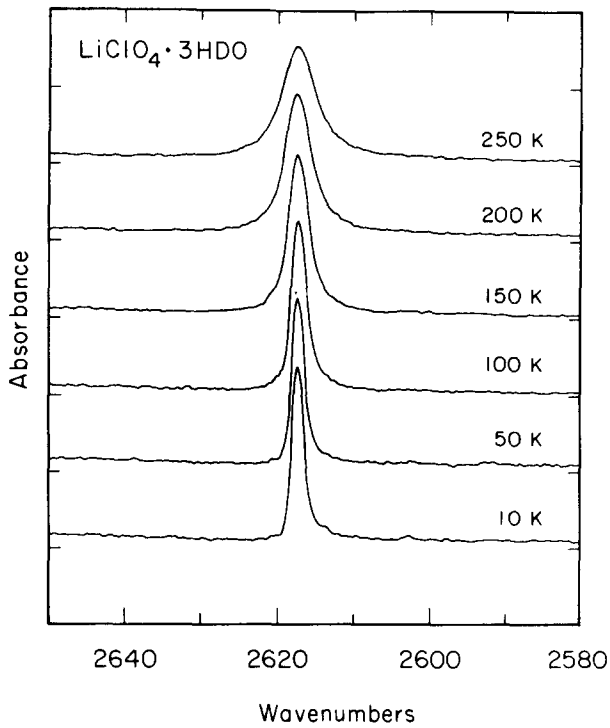

FIG. 1. The infrared spectrum of the OD stretch of a dilute sample of HDO in $LiClO_4 \cdot 3H_2O$, as a function of temperature. A very small band due to HDO^{18} in natural abundance appears at 2602 cm^{-1}.

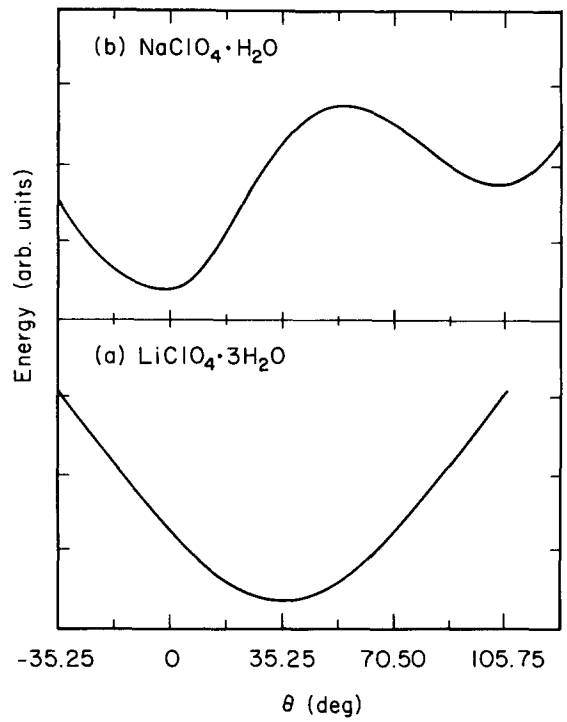

FIG. 2. The electrostatic energy of water of hydration as a function of librational angle. (a) $LiClO_4 \cdot 3H_2O$, (b) $NaClO_4 \cdot H_2O$. The energy scale is arbitrary.

culations as well as with the neutron diffraction results.[10] $LiClO_4 \cdot 3H_2O$ has six equivalent water molecules in a unit cell.[10] The electrostatic energy as a function of the position of one water per unit cell (with the others in the symmetric position) shows a single minimum at $\theta = 35.25°$, the position which preserves the plane of symmetry through the water oxygen (Fig. 2). This single minimum occurs for all hydrogen atom charges from $+0.5e$ to $+1.0e$.

No large amplitude motion occurs in $LiClO_4 \cdot 3H_2O$. The widths of the bands in this crystal are due to a variety of other unspecified mechanisms, presumably inhomogeneous broadening at low temperature and both homogeneous and inhomogeneous broadening at higher temperatures. We assume that these same mechanisms operate for the other hydrates and subtract the "$LiClO_4 \cdot 3H_2O$ contribution" from their linewidths to isolate the effect of the large amplitude motion.

B. $NaClO_4 \cdot H_2O$

1. *Infrared spectra*

The OD stretching region of isotopically dilute $NaClO_4 \cdot H_2O$ at 7 K is shown in Fig. 3 and Table I. The two large peaks at 2604.5 and 2646.5 cm^{-1} are the OD stretching bands of HDO. They collapse and broaden with temperature as displayed in Fig. 4. The two bands at low temperature correspond to two different sites for the OD bond. It is well known that OH (and OD) stretches gain intensity and drop in frequency as the hydrogen bond becomes stronger. This correlation accounts for the asymmetric nature of the low temperature spectra in Figs. 3 and 4 which show the lower frequency band to be stronger than the high frequency one. The line shifts and linewidths are smooth functions of temperature but unlike the band in $LiClO_4 \cdot 3H_2O$ they change considerably from 7 to 50 K. The line shifts are listed in Table II and plotted in Fig. 5. The linewidths of the two OD stretches at various temperatures are

TABLE I. Low temperature (7 K) frequencies (in cm^{-1}).

Crystal	$O^{16}D$(HDO)	$O^{18}D$(HDO)	$\nu_3(D_2O)$	$\nu_1(D_2O)$	HOD bend
$LiClO_4 \cdot 3H_2O$	2617.4	2602.5			1438.1
$NaClO_4 \cdot H_2O$	2604.5	2589.9	2673.8[a]	2582.9	1413.9
	2646.4	2631.8			1430.1
$LiI \cdot 3H_2O$	2527.0	2512.9	2670.8	2518.2[b]	1395.7
	2651.5	2636.9		2532.2	1420.8
				2531.7	

[a]Broad, possible Fermi resonance. [b]Fermi resonance.

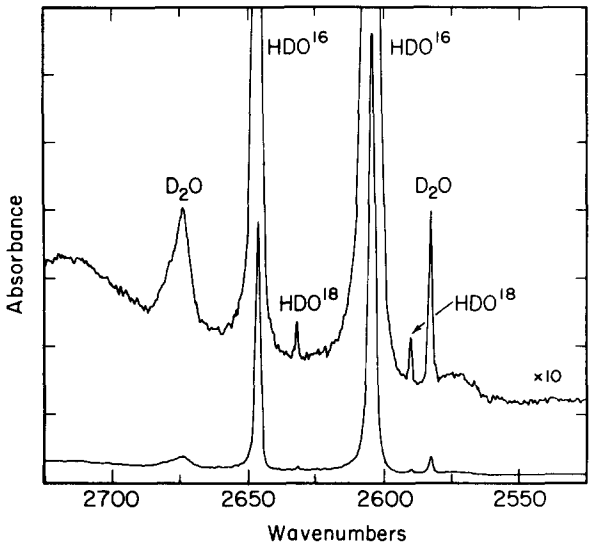

FIG. 3. The infrared spectrum of the OD stretching region of $NaClO_4 \cdot H_2O$ under similar conditions as Fig. 1. Spectrum at 7 K.

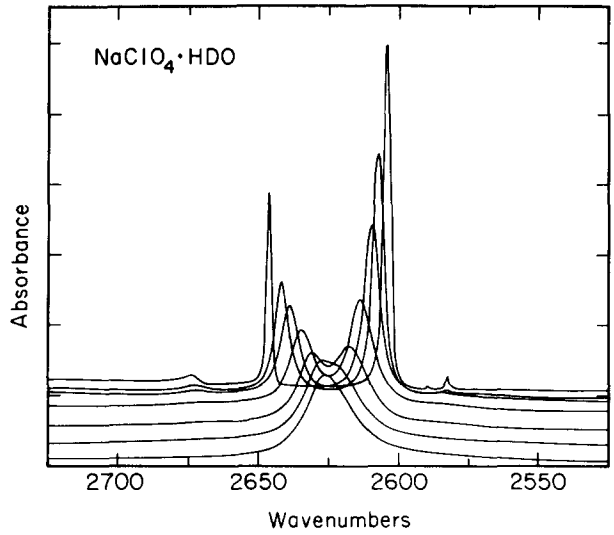

FIG. 4. Temperature dependence of the OD stretching band to $NaClO_4 \cdot H_2O$. The spectra are at 10, 70, 100, 175, 200, 250, and 290 K. Compare to Figs. 1 and 3.

listed in Table III. The exchange process responsible for the band collapse is only one of a number of possible mechanisms which could give rise to a temperature dependence of the linewidths. As a first attempt to account for these other effects, we have corrected the linewidths in the following fashion: the linewidth of the band in $LiClO_4 \cdot 3H_2O$ is normalized to have the same low temperature linewidth as the $NaClO_4 \cdot H_2O$ band in question, and that value is subtracted from the experimentally observed linewidths to obtain the broadening as a function of temperature. The logarithm of this corrected broadening is plotted against $1/T$ in Fig. 6. Greater scatter in the data is observed at higher temperatures; this is due to the greater uncertainties in the deconvolutions of the more strongly overlapped peaks.

The small bands at 2673.8 and 2582.9 cm^{-1} in Fig. 3 are the antisymmetric and symmetric stretching modes of isotopically dilute D_2O. Note that the asymmetric stretch is considerably broader than the symmetric stretch; this is possibly due to a Fermi resonance. The assignment of these bands to D_2O was verified by increasing the amount of deuterium in the sample. These two bands move towards each other only 6.5 cm^{-1} from 7 to 250 K.

The two smallest bands in Fig. 3 at 2631.8 and 2590.0 cm^{-1} are the two $O^{18}D$ stretches of HDO.[18] The intensities are approximately correct for the 0.2% natural abundance of O^{18} and the ability to see them at all attests to the sensitivity of the technique. The isotope shift for both bands is 14.9 cm^{-1}, which is consistent with simple mass factor calculations and with HDO^{16}–HDO^{18} shifts observed in matrix isolation studies.[22] The presence of the two HDO^{18} bands at the expected positions shows that the OD splitting is really due to two distinct sites and eliminates Fermi resonance and factor group splitting from consideration. The latter follows since the amount of HDO^{18} is only 0.2% of the already small HDO concentration and so the number of unit cells containing two HDO^{18} is negligible.

The HDO bending region also exhibits two bands which

TABLE II. HDO^{16} stretching frequency line shifts (in cm^{-1}).

	$NaClO_4 \cdot H_2O$[a]				$LiI \cdot 3H_2O$	
T (K)	$\Delta\omega_a$	$\Delta\omega_a$(calc.)	$-\Delta\omega_b$	$-\Delta\omega_b$(calc.)	$\Delta\omega_a$	$-\Delta\omega_b$
20	0.2		0.4			0.6
50	1.6	1.6	2.8	2.8	0.1	2.9
70	2.9	2.6	4.8	4.3		
75					1.0	5.5
100	5.1	3.6	7.5	5.7	2.2	8.4
125	7.1	4.1	9.9	6.4	4.1	11.7
150	8.9	4.5	12.0	6.9	6.2	15.3
175	11.2	4.7	14.0	7.2	9.6	19.3
200	13.3	4.9	15.5	7.5		
225	15.9	5.1	18.5	7.7		

[a]The calculations take into account the in-plane libration only. The remainder of the shift is due to the flipping motion.

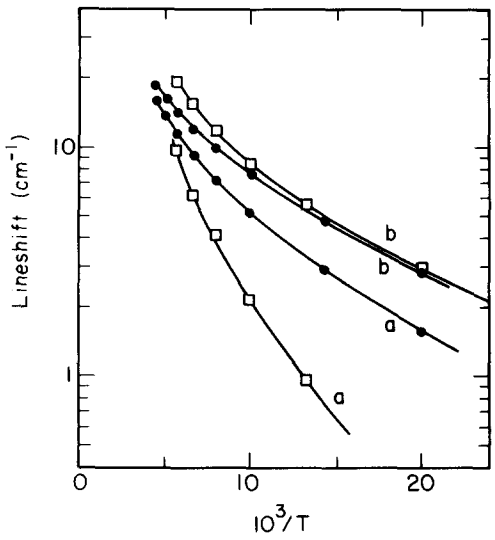

FIG. 5. The line shfits of the a and b OD stretching bands of $NaClO_4 \cdot H_2O$ (circles) and $LiI \cdot 3H_2O$ (squares). In this figure and Fig. 9 the negative of the line shift for line b is plotted for convenience.

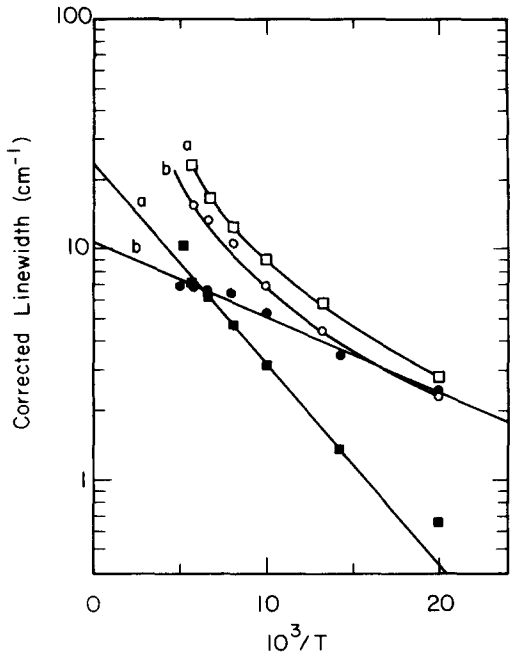

FIG. 6. The linewidths of the a and b OD stretching bands of $NaClO_4 \cdot H_2O$ and $LiI \cdot 3H_2O$. The widths have been corrected by subtracting the scaled width of the corresponding $LiClO_4 \cdot 3H_2O$ band (Table III). The dark squares and circles are for $NaClO_4 \cdot H_2O$, the open data points are for $LiI \cdot 3H_2O$.

collapse with temperature (Table IV). The collapse of the two bands is superimposed upon a shift to higher frequency with increasing temperature; for comparison the shift of the HOD bend in $LiClO_4 \cdot 3H_2O$ is also listed in Table IV. The change in the splitting of the $NaClO_4 \cdot H_2O$ bend as a function of temperature is similar to that of the OD stretch.

2. Potential function

The water in $NaClO_4 \cdot H_2O$ sits in a site of C_1 symmetry [Fig. 7(a)]. The electrostatic energy calculation reveals two minima of unequal energy [Fig. 2(b)]. As mentioned above, the absolute energy difference between the two minima cannot be ascertained from the calculation. We assume, however, that the ratio of the barrier height to this energy difference and the θ positions of the two minima are correctly given by the potential, and we fit a simple analytic potential function of the form

$$V(\theta) = a\theta^2 + b\theta^3 + c\theta^4 \ . \tag{1}$$

The advantage of this potential is that once the constants are determined, the energy levels and corresponding wave functions can be easily calculated from a perturbation calculation using a harmonic oscillator basis set.[23] For all of our calculations, we include the first 20 energy levels in the perturbation matrix.

The potential function (1) is shown in Fig. 8. The ratio $V^*/\Delta V$ and $\Delta\theta$ are taken from the electrostatic calculation with $+1.0e$ H atom charge (these numbers

TABLE III. HDO^{16} stretches–linewidths (in cm^{-1}).

		$NaClO_4 \cdot H_2O$						$LiI \cdot 3H_2O$			
			Line a			Line b			Line a		Line b
T(K)	$LiClO_4 \cdot 3H_2O$[a]	Line a	(corrected)	τ_c[b]	Line b	(corrected)	τ_c	Line a	(corrected)	Line b	(corrected)
10	...	...	...	...	0.04	0.04	...	0.10	0.10	0.16	0.16
20	...	...	...	...	0.41	0.41	...	0.35	0.35	0.54	0.54
50	0.15	0.9	0.65	0.37	2.5	2.38	0.78	2.9	2.8	2.4	2.35
70	0.25	1.8	1.35	0.57	3.7	3.45	0.90	6.2[c]	5.8	4.6	4.4
100	0.40	3.7	3.15	1.2	5.7	5.26	1.3	9.6	8.9	7.2	6.9
125	0.80	5.9	4.7	1.8	7.3	6.45	1.6	13.6	12.5	11.0	10.5
150	1.20	7.8	6.1	2.4	7.7	6.5	1.7	18.4	16.5	13.9	13.1
175	1.65	9.5	7.1	3.0	8.7	7.0	1.4	25.9	23.2	16.6	15.4
200	2.10	13.1	10.3	4.5	8.7	7.0	2.0				
225	2.83	14.8	10.7	4.9	10.1	7.2	2.2				
250	3.45	15.4	10.5		9.8	6.2					
293	4.85										

[a]These values were scaled and used to correct the widths of the $NaClO_4 \cdot H_2O$ and $LiI \cdot 3H_2O$ line.
[b]In ps.
[c]$LiI \cdot 3H_2O$ is at 75 K instead of 70 K.

TABLE IV. HDO bends—positions and splittings (in cm^{-1}).

T (K)	ν_2 $LiClO_4 \cdot 3H_2O$	$\Delta\nu_2$ $NaClO_4 \cdot H_2O$	$\Delta\nu_2$ $LiI \cdot 3H_2O$
7	1438.1	16.2	25.1
10		16.2	25.1
20		16.0	25.1
50	1438.1	14.2	24.5
70		13.4	23.7
100	1438.8	11.2	22.5
125	1439.2	9.3	20.4
150		6.9	13.8
175		4.4	14.9
200	1440.2	a	a
250	1441.7	a	a

[a]The bands are too badly overlapped to determine the splitting.

are not very sensitive to the H atom charge); one more constant is required. We will use this constant in the next section to adjust the energy scale to fit the experimental line shifts.

3. Line shift calculations

At the lowest temperatures, two OD stretches are observed for HDO molecules in $NaClO_4 \cdot H_2O$. This is

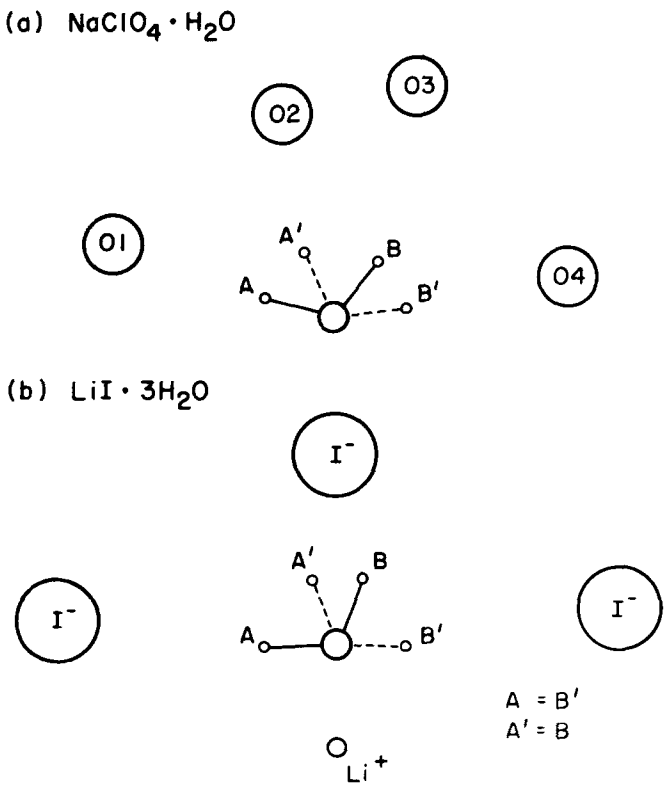

FIG. 7. Diagram of the water sites in (a) $NaClO_4 \cdot H_2O$ and (b) $LiI \cdot 3H_2O$. The diagrams are projections of the atomic positions onto the plane of the water molecule. Only the oxygen atoms closest to the water in the $NaClO_2 \cdot H_2O$ are shown. The atoms O2 and O3 in the $NaClO_4 \cdot H_2O$ and the Li^+ ion and the central I^- ion in the $LiI \cdot 3H_2O$ are not in the plane. The $NaClO_4 \cdot H_2O$ site has no symmetry perpendicular to the plane of the diagram while the $LiI \cdot 3H_2O$ site has a plane of symmetry going through the water. Possible sites for an OD bond are labeled; the heavy atom positions are from Refs. 7 and 11.

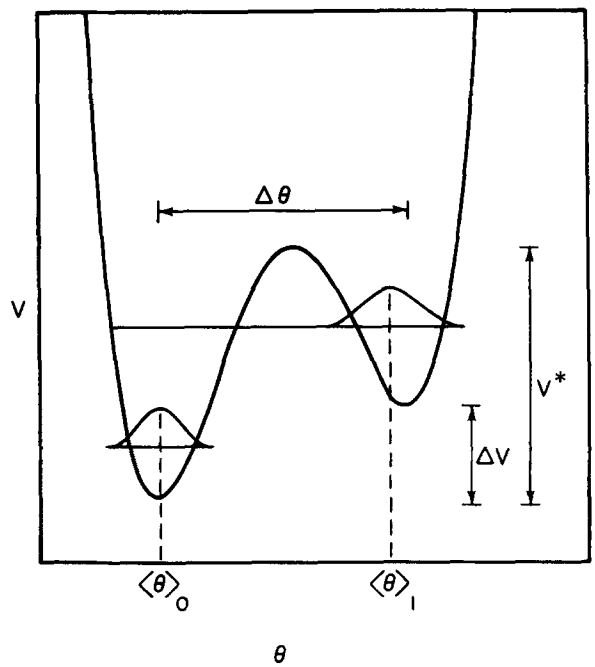

FIG. 8. The asymmetric double minimum potential for $NaClO_4 \cdot H_2O$. The two lowest librational wave functions are sketched and their average values of θ denoted. The values of $\Delta\theta$, ΔV, and V^* determine the potential function of Eq. (1).

what one would expect from the potential in Fig. 8. The ground state for the water molecule has an average θ position $\langle\theta\rangle_0$ corresponding to the unprimed "site" in Fig. 7. There are two inequivalent hydrogen positions labeled A and B; an HDO molecule can sit with its deuterium in either position. A 180° flip is required to exchange these two positions; this is a slow process (with a barrier on the order of kcal per mol) which freezes out, leaving a nonequilibrium distribution as the crystal is cooled. The two positions have OD stretching frequencies $\langle\omega_a\rangle_0$ and $\langle\omega_b\rangle_0$ (the zero refers to the ground librational state). Since position A has a shorter, more linear hydrogen bond, we expect $\langle\omega_a\rangle_0$ to be less than $\langle\omega_b\rangle_0$.

Now consider raising the temperature of the crystal. There are two types of HDO molecules in the hydrate. HDO molecules with a deuterium in position A see a net increase in their stretching force constant as it is averaged over the librational potential; the infrared band $\langle\omega_a\rangle$ is correspondingly shifted upwards in frequency. The opposite occurs for HDO molecules with a deuterium in position B; they feel a net decrease in their OD stretching force constant, so that $\langle\omega_b\rangle$ is shifted down in frequency. The overall effect is an apparent collapse of the two OD bands.

To calculate this collapse we separate the total Hamiltonian into three parts

$$H_{\text{tot}} = H_V + H_L + H_{LV} \,, \tag{2}$$

where H_V is the Hamiltonian for the stretching vibration of the HDO, H_L is the libration Hamiltonian, and H_{LV} is the interaction Hamiltonian between the two. The statistically averaged effect of H_{LV} on H_V is described by

the Redfield exchange theory.[13] In the limit of motional narrowing of the librations, the OD stretching spectral positions are thermally weighted averages over these lower energy levels. We shall not treat the coupling between the bath and the libration explicitly, but simply assume that the librational modes are undergoing fluctuations about thermal equilibrium. We further assume that we are in the motional narrowing limit and that correlation functions of the libration are characterizable by relaxation times.

We now calculate the energy levels of H_{tot} ignoring the fluctuations in H_L and H_{LV}, i.e., the time independent energy levels. Note that H_{tot} is different for an HDO with its deuterium in site A from an HDO with the deuterium in site B. For the former case the parts of H_{tot} are given by Eqs. (3)–(5):

$$H_V\,|\,\psi_n^\circ(q_a)\rangle = (T_V + \tfrac{1}{2}m\omega_a^{\circ 2}q_a^2)\,|\,\psi_n^\circ\rangle = \hbar\omega_a^\circ(n+\tfrac{1}{2})\,|\,\psi_n^\circ\rangle\ , \tag{3}$$

$$H_L\,|\,\phi_p^\circ(\theta)\rangle = (T_L + V_L)\,|\,\phi_p^\circ\rangle = \epsilon_p^\circ\,|\,\phi_p^\circ\rangle\ , \tag{4}$$

$$H_{LV} = m\omega_a^\circ\delta\omega_a(\theta)q_a^2\ . \tag{5}$$

Analogous equations apply for HDO molecules with a deuterium in site B. The constant m in Eqs. (3) and (5) is an effective mass; q_a is the stretching coordinate. V_L in Eq. (4) is the potential of Eq. (1) and is the same for both types of HDO molecules. The other symbols have their usual meanings or are defined by the equations.

We solve Eq. (2) in the limit in which $\delta\omega_a(\theta) \ll \omega_a^\circ$. In this limit, the adiabatic approximation[24] is valid, and the wave functions of H_{tot} can be written as the product of a vibrational and a librational part

$$|\,\Phi_{n,p}\rangle = |\,\psi_n\rangle\,|\,\phi_p\rangle\ , \quad \begin{matrix} p=0,1,2,\ldots \\ n=0,1,2,\ldots \end{matrix}\ , \tag{6}$$

and

$$E_{n,p}^a = \epsilon_p^\circ + \hbar\omega_a^\circ(n+\tfrac{1}{2}) + \hbar\langle\delta\omega_a\rangle_p(n+\tfrac{1}{2})\ , \tag{7}$$

where

$$\langle\delta\omega_a\rangle_p \equiv \langle\phi_p^\circ\,|\,\delta\omega_a(\theta)\,|\,\phi_p^\circ\rangle\ .$$

The librational frequencies $\langle\Omega_a\rangle_p$ and the stretching vibrational frequencies $\langle\omega_a\rangle_p$ are

$$\langle\Omega_a\rangle_p \equiv \frac{E_{0,p}^a - E_{0,0}^a}{\hbar} = \Omega_p^\circ + \tfrac{1}{2}(\langle\delta\omega_a\rangle_p - \langle\delta\omega_a\rangle_0)\ , \tag{8}$$

where

$$\Omega_p^\circ \equiv \frac{\epsilon_p^\circ - \epsilon_0^\circ}{\hbar}\ ,\quad p=1,2,\ldots\ ,$$

$$\langle\omega_a\rangle_p \equiv \frac{E_{1,p}^a - E_{0,p}^a}{\hbar} = \omega_a^\circ + \langle\delta\omega_a\rangle_p\ ,\quad p=0,1,2,\ldots\ , \tag{9}$$

with similar formulas for position B.

We are now in a position to calculate the line shifts. At sufficiently low temperatures, only the two lowest librational levels are populated and the line shifts $\langle\overline{\omega_a}\rangle - \langle\omega_a\rangle_0$ and $\langle\overline{\omega_b}\rangle - \langle\omega_b\rangle_0$ are simple exponential functions (in the following formulas $\langle\overline{\omega_a}\rangle$ and $\langle\overline{\omega_b}\rangle$ represent statistical averages while the remaining quantities are simple quantum mechanical averages)

TABLE V. Libration and stretching frequencies as a function of librational state.

Librational state	Librational frequencies (cm^{-1})				Vibrational frequencies (cm^{-1})	
p	Ω_p^0	$\langle\Omega_p^a\rangle$	$\langle\Omega^b\rangle_p$	$\langle\theta\rangle_p$	$\langle\omega_a\rangle_p$	$\langle\omega_b\rangle_p$
0	...	...	...	88°	2604.5	2446.4
1	64	68	60	37°	2615.5	2629.9
2	97	100	95	59°	2608.7	2640.1
3	153	157	147	66°	2612.0	2635.2
4	218	221	213	55°	2611.0	2637.0
5	292	295	287	55°	2611.0	2637.0
6	374	377	369	55°	2611.0	2637.0
7	462	465	457	55°	2611.0	2637.0
8	560	563	555	55°	2611.0	2637.0

$$\begin{aligned}\langle\overline{\omega_a}\rangle - \langle\omega_a\rangle_0 &= (\langle\omega_a\rangle_1 - \langle\omega_a\rangle_0)\exp(-\hbar\langle\Omega_a\rangle_1/kT) \\ &= 2(\langle\Omega_a\rangle_1 - \Omega_1^\circ)\exp(-\hbar\langle\Omega_a\rangle_1/kT)\ , \\ &\quad \text{for } kT \ll \hbar\langle\Omega_a\rangle_1\ .\end{aligned} \tag{10}$$

$$\begin{aligned}\langle\overline{\omega_b}\rangle - \langle\omega_b\rangle_0 &= (\langle\omega_b\rangle_1 - \langle\omega_b\rangle_0)\exp(-\hbar\langle\Omega_b\rangle_1/kT) \\ &= 2(\langle\Omega_b\rangle_1 - \Omega_1^\circ)\exp(-\hbar\langle\Omega_b\rangle_1/kT)\ , \\ &\quad \text{for } kT \ll \hbar\langle\Omega_b\rangle_1\ .\end{aligned} \tag{11}$$

Here, $\langle\omega_a\rangle_0$ and $\langle\omega_b\rangle_0$ are the frequencies of the OD stretches at the lowest temperature. The constants $\langle\omega_a\rangle_1$, $\langle\omega_b\rangle_1$, $\langle\Omega_a\rangle_1$, and $\langle\Omega_b\rangle_1$ can be determined from the low temperature slopes and intercepts of the line shifts. The energy difference between the first two levels of V_L, $\hbar\Omega_1^\circ$, is found from Eqs. (10) and (11) and the data to be 65 ± 15 cm^{-1}.

This energy difference is the third parameter needed to define the asymmetric double minimum potential [Eq. (1)]. As stated in the previous section, once the potential is fixed, all the librational energy levels and wave functions can be calculated. To make use of this we expand the coupling $\delta\omega_a(\theta)$ and truncate it after the term linear in θ:

$$\langle\delta\omega_a\rangle_p \cong \delta\omega_a^\circ + \delta\omega_a'\langle\theta\rangle_p\ , \tag{12}$$

$\delta\omega_a^\circ$ and $\delta\omega_a'$ are constants whose values are determined from $\langle\omega_a\rangle_1$, $\langle\omega_a\rangle_0$, $\langle\theta\rangle_1$, and $\langle\theta\rangle_0$. The latter two averages are calculated from the wave functions obtained from the librational potential.

From Eq. (12), the line shift as a function of temperature follows immediately:

$$\langle\overline{\omega_a}\rangle - \langle\omega_a\rangle_0 = \frac{\langle\omega_a\rangle_0 + \sum_{p=1}^\infty \langle\omega_a\rangle_{p+1}\exp(-\hbar\langle\Omega_a\rangle_p/kT)}{1 + \sum_{p=1}^\infty \exp(-\hbar\langle\Omega_a\rangle_p/kT)}\ , \tag{13}$$

where $\langle\omega_a\rangle_p$ and $\langle\Omega_a\rangle_p$ are given by Eqs. (8) and (9). The calculated line shifts are tabulated along with the experimental values in Table II. The sums in Eq. (13) were taken out to $p=5$; the various constants for the first five librational levels are given in Table V.

The calculated line shifts listed in Table II deviate from the observed line shifts at higher temperatures. The simple Boltzmann average over the librational potential predicts that the line positions should approach their high temperature averages. As the curves in Fig.

5 show, however, the rate of line shift *increases* at higher temperatures. This indicates the onset of some higher energy exchange process, probably the 180° flipping mode. The contribution to the line shift by this process is obtained by subtracting the calculated line shift from the observed line shifts. This difference is plotted semilogarithmically versus $1/T$ in Fig. 9. The line shifts for both the a and the b bands lie on the same curve, as they should if the 180° flip is this higher temperature exchange process. The curve is straight and yields a slope of 220 cm^{-1}. Application of the low temperature limits [Eqs. (10) and (11)] of the Redfield averaging theory to this second exchange process identifies this number as the energy splitting between the first two energy levels of the potential function for the 180° flip. By assuming a simple $\cos 2\theta$ potential this splitting corresponds to a barrier height of from 6 to 10 kcal/mol depending on what value of the reduced mass is chosen. This value of the barrier is in agreement with the quadrupole resonance results (little averaging at −55 °C and rapid averaging compared to 5 kHz at 25 °C) and is of the same order as other H_2O flipping barriers.[25]

4. Linewidth calculation

In addition to predicting the line shifts for $NaClO_4 \cdot H_2O$, the Redfield theory also gives the linewidths of the two OD stretches $-2R^a_{1010}$ and $-2R^b_{1010}$, in terms of the root-mean-square fluctuations in the librational angle (see Appendix A):

$$-2R^a_{1010} = \sqrt{2\pi}\,(\delta\omega'_a)^2[\overline{\langle\theta\rangle^2} - (\overline{\langle\theta\rangle})^2]\tau_c\,, \tag{15}$$

$$-2R^b_{1010} = \sqrt{2\pi}\,(\delta\omega'_b)^2[\overline{\langle\theta\rangle^2} - (\overline{\langle\theta\rangle})^2]\tau_c\,, \tag{16}$$

where τ_c is the phenomenological correlation time for the librational motion. The temperature dependence of the linewidths arises from the changes in the thermal averages and from the temperature dependence of τ_c. The thermal averages are easily determined from the values calculated for the energy levels listed in Table V. From these averages and the corrected linewidths we have calculated τ_c as a function of temperature and have listed the values in Table III. τ_c varies from ~1–10 ps; this agrees with the motional narrowing assumptions made in the Redfield theory.

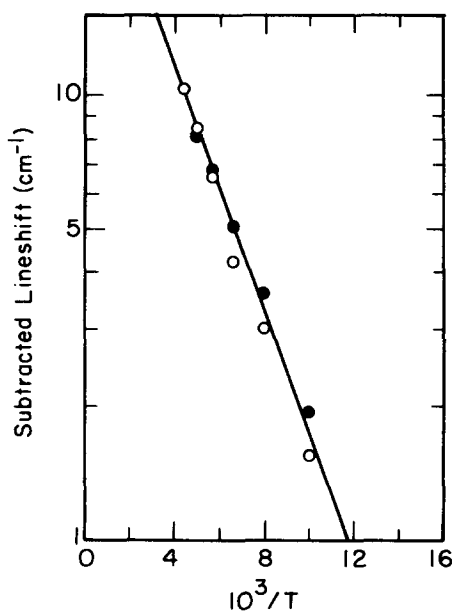

FIG. 9. Line shift of the OD stretching bands in $NaClO_4 \cdot H_2O$ due to the high temperature flipping motion. The open circles are the shifts of the a line, the dark circles are the shifts from the b line. The slope corresponds to an energy of 220 cm^{-1}.

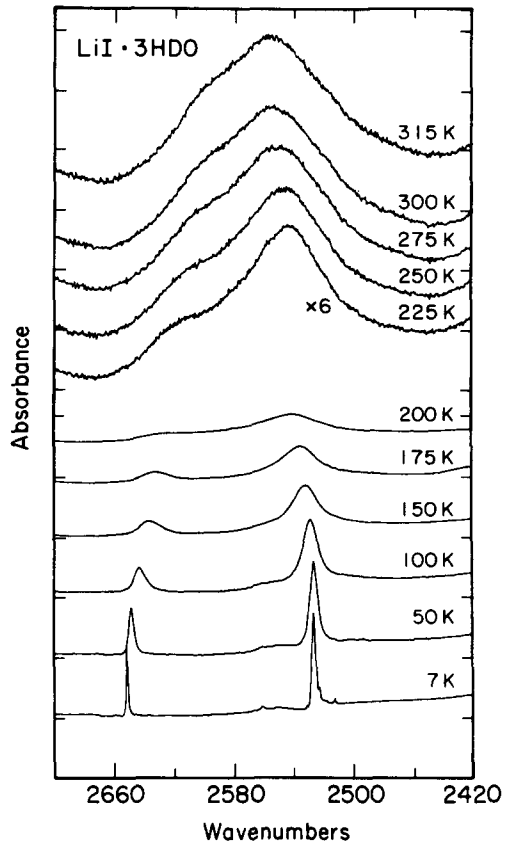

FIG. 10. The OD stretching region of $LiI \cdot 3H_2O$ under conditions similar to Fig. 1. The lowest temperature spectrum shows small bands due to HDO^{18} and D_2O (see Table I for the frequencies). Additional HDO combination bands appear at 2550, 2560, 2603, 2623, and 2658 cm^{-1}.

C. $LiI \cdot 3H_2O$

1. Infrared spectra

The low temperature spectrum of $LiI \cdot 3H_2O$ (Fig. 10) shows more structure in the OD stretching region than does the spectrum of $NaClO_4 \cdot H_2O$. Two $O^{18}D$ stretches and their $O^{18}D$ counterparts are observed. Increasing the deuterium concentration reveals the D_2O bands; we find that the ν_1 band is split by a Fermi resonance with the D_2O bending vibration.[26] In addition there are a number of bands which scale as the HDO molecules with deuterium concentration. We tentatively assign them to combinations of the OD fundamental with translational and librational modes.

The two OD stretches collapse as a function of temperature (Fig. 10), but with marked differences from the $NaClO_4 \cdot H_2O$ case. At lower temperatures, the two line shifts have considerably different slopes (Fig. 5),

unlike the line shifts in $NaClO_4 \cdot H_2O$. Moreover, the bands broaden tremendously upon collapse (Table III).

The HDO bends in $LiI \cdot 3H_2O$ are not as widely split as the stretches at low temperature and overlap more quickly. The change in splitting versus $1/T$ (Table IV) is of the same form as all the other observed collapses.

2. *Potential calculation and symmetry breaking*

The large splittings observed in the infrared spectra of $LiI \cdot H_2O$ are quite surprising in view of its crystal structure. The water arrangement in $LiI \cdot 3H_2O$ is very similar to that in $LiClO_4 \cdot 3H_2O$.[12] As in $LiClO_4 \cdot 2H_2O$, there is a plane of symmetry through the water oxygen [Fig. 7(b)]. No neutron diffraction study has been made on the crystal, so like Falk[12] we assume that the water molecule is in the same plane as the water molecules in $LiClO_4 \cdot 3H_2O$. Thus, the crystal symmetry forces the librational potential to be symmetric about $\theta = 35.25°$. In fact, the electrostatic energy for moving one water per unit cell exhibits a single minimum at $\theta = 35.25°$, just as for $LiClO_4 \cdot 3H_2O$.

However, the low temperature spectra show that the symmetry is definitely broken. Following the suggestion of Brink and Falk,[12] we explored the possibility that the symmetry is lowered from $P6_3mc$-C_{6v}^4 at high temperature to $P6_3$-C_6^6 at low temperature. The lower symmetry corresponds to moving all six water molecules per unit cell simultaneously to the right or left [all to the A–B or all to the A′–B′ positions in Fig. 7(b) simultaneously]. The water molecules form an octahedron about the Li^+ ions and at the same time a distorted octahedron about the I^- ions. Moving the waters "left" or "right" together involves the least breaking of the original crystal symmetry. This leaves all the water molecules equivalent, while removing the symmetry plane that otherwise bisects each water molecule. With a charge of $+0.7e$ on the water hydrogens, this motion leads to a calculated double minimum for $LiI \cdot 3H_2O$ but *not* for the very similar $LiClO_4 \cdot 3H_2O$. The coupled motion breaks the symmetry about the water molecule and gives rise to the doubled OD stretching and HDO bending bands. Note that the collective motion is subtle; our electrostatic calculation automatically moves all the images of a given molecule in different unit cells together, and so the distinction between moving one water per unit cell or six is one that involves nearest neighbors. Presumably the water molecules form right and left domains, but we did not try to model the domain size in our calculation.

Our picture of the structure of $LiI \cdot 3H_2O$ as a function of temperature is as follows. At high temperature, the thermal motion of each water molecule occurs more or less independently, giving a crystal with a plane of symmetry through the water and only one HDO stretching and one HDO bending vibrational band.

As the temperature is lowered, the flipping libration which would exchange the positions of the H and the D freezes out. At lower temperatures still, the correlation between the in-plane librations of adjacent water molecules increases and results in domains with a given HDO trapped with its deuterium in either the A or B position [Fig. 7(b)].[27] The infrared splitting of the OD stretching bands should provide a measure of the extent of position correlation of the waters as a function of temperature. In the absence of much more detailed calculations, we can come only to the qualitative conclusion that the in-plane librational correlation seems to decrease gradually with temperature and still persists to some extent even at room temperature (Fig. 10).

V. SUMMARY AND CONCLUSIONS

It is clear that the motions of water in weakly bound hydrates are highly dependent on the exact geometry and size of the water site. In $LiClO_4 \cdot 3H_2O$, the water sits in a well-defined site which exhibits a deep single energy minimum as a function of the librational coordinate. The well-defined position of the water leads to straightforward x-ray and neutron diffraction determination. In this paper, we have shown that the use of very dilute HDO yields narrow OD stretching and HOD bending bands at all temperatures for the well-defined water. The OD stretching band also remains at a constant frequency. A simple electrostatic calculation reproduces the single minimum position deduced from the structural and infrared data.

The same techniques applied to $NaClO_4 \cdot H_2O$ show a very different situation. The OD stretching bands narrow dramatically and split at low temperature. The electrostatic calculations provide a double minimum potential that fits the observations. We have shown that the use of the Redfield equations which assume the rapid decay of correlations among the librational levels leads to a detailed description of both the line shifts and linewidths. All of this leads to a picture of the water molecule librating with increasingly greater amplitude in its plane as the temperature is increased. At higher temperature, still the water flips rapidly and exchanges the hydrogen positions. This sequence of motions explains all the structural and spectroscopic data available.

The third case we examined $LiI \cdot 3H_2O$ represents a long standing mystery. The x-ray data suggest a crystal with a plane of symmetry through the water just as in $LiClO_4 \cdot 3H_2O$. The infrared spectra prove the contrary, at least at low temperature. The electrostatic calculations resolve the problem. An asymmetric structure results if the water molecules move in a phased fashion. A quantitative explanation of the infrared spectra requires a detailed understanding of this phased motion in order to apply the Redfield equations; this is a project we leave to the future.

Our method of analyzing the vibrational spectra should be generally applicable. Application of the Redfield assumptions leads to the observed high frequencies (such as that for O–D stretching) being just averages over the low frequency motions (such as the librations). The widths of the bands are just root-mean-square averages over the motions whose exact forms will depend on the detailed nature of the high frequency motion–low frequency motion coupling. In the low temperature limit, our formulas reduce to those of the two level hot band dephasing model of Shelby *et al.*[29] and similar models.[30]

However, our equations are applicable for all temperatures and for more complex situations[14] as long as the basic assumptions are met.

ACKNOWLEDGMENTS

We thank the National Science Foundation for support. Professor Robert A. Harris' advice has been deeply appreciated, and we thank Professor David Templeton for suggesting and explaining Bertaut's method for electrostatic calculations. The interest and encouragement of Dr. Robert G. Snyder and Dr. Richard A. MacPhail has been invaluable.

APPENDIX A: LINEWIDTH CALCULATION FOR $NaClO_4 \cdot H_2O$

We follow the standard Redfield prescription[13,14] and define

$$H_0 = T_v + \tfrac{1}{2} m\omega_a^2 q_a^2 + m\omega_a^\circ \overline{\langle \delta\omega_a \rangle}\, q_a^2 \tag{A1}$$

and

$$H_1 = m\omega_a^\circ [\delta\omega_a(\theta) - \overline{\langle \delta\omega_a \rangle}] q_a^2 , \tag{A2}$$

where T_v is the vibrational kinetic energy, m is the effective mass, ω_a° the time and libration independent stretching frequency of the HOD in the "A" position, and q_a the corresponding normal coordinate. $\delta\omega_a(\theta)$ is the contribution to the stretching frequency that varies with the librational angle and of course $\overline{\langle \delta\omega_a \rangle}$ is its quantum and statistical average value. The stretching energy levels are

$$E_n^a = \hbar\omega_a^\circ (n + \tfrac{1}{2}) + \hbar \overline{\langle \delta\omega_a \rangle} (n + \tfrac{1}{2}) , \tag{A3}$$

with formulas similar to (A1), (A2), and (A3) for position B. To calculate the linewidths we need the time dependence of the (1, 0) density matrix element for the stretching energy levels.[28] With the assumption that the librational levels relax rapidly enough (to be justified *a posteriori*), we find we need only the Redfield relaxation matrix element

$$R_{1010} = \frac{1}{2\hbar^2} [2J_{1100}(0) - J_{1111}(0) - J_{0000}(0)] , \tag{A4}$$

where

$$J_{abcd}(\omega) = \int_{-\infty}^{\infty} d\tau\, e^{-i\omega\tau} \overline{\langle a | H_1(t) | b \rangle \langle c | H_1(t+\tau) | d \rangle} . \tag{A5}$$

With

$$\begin{aligned} \langle 0 | H_1 | 0 \rangle &= \tfrac{1}{2}\hbar [\delta\omega_a(\theta) - \overline{\langle \delta\omega_a \rangle}] , \\ \langle 1 | H_1 | 1 \rangle &= \tfrac{3}{2}\hbar (\delta\omega_a - \overline{\langle \delta\omega_a \rangle}) , \\ \langle 0 | H_1 | 1 \rangle &= 0 , \end{aligned} \tag{A6}$$

Eq. (A4) reduces to

$$R_{1010} = -\frac{1}{2} \int_{-\infty}^{\infty} C(\tau)\, d\tau , \tag{A7}$$

where we defined the correlation function given in Eq. (A8)

$$C(\tau) = \overline{[\delta\omega_a(0) - \overline{\langle \delta\omega_a \rangle}][\delta\omega_a(\tau) - \overline{\langle \delta\omega_a \rangle}]} . \tag{A8}$$

With the linear coupling assumption to Eq. (12), this correlation function becomes

$$C(\tau) = (\delta\omega_a')^2 [\theta(0)\theta(\tau) - (\langle \bar{\theta} \rangle)^2] . \tag{A9}$$

We now take a simple exponential form for the librational correlation function of Eq. (A9) and obtain

$$R_{1010}^a = -\frac{\sqrt{2\pi}}{2} (\delta\omega_a')^2 [\overline{\langle \theta \rangle^2} - (\langle \bar{\theta} \rangle)^2] \tau_c ,$$

where τ_c is the correlation time for the libration. This leads directly to Eqs. (15) and (16).

[1] J. Schiffer and D. F. Hornig, J. Chem. Phys. **49**, 4150 (1968).
[2] M. Falk and O. Knop, in *Water: A Comprehensive Treatise*, edited by F. Franks (Plenum, New York, 1973), Vol. 2, Chap. 2.
[3] L. W. Reeves, in *Progress in NMR Spectroscopy*, edited by J. W. Emsley, J. Feeney, and L. H. Sutcliffe (Pergamon, New York, 1969), Vol. 4, Chap. 3.
[4] See Ref. 2, p. 88.
[5] H. J. Hrostowski and G. C. Pimentel, J. Chem. Phys. **19**, 661 (1951); G. L. Hiebert and D. F. Hornig, *ibid.* **20**, 918 (1952).
[6] G. Brink and M. Falk, Can. J. Chem. **48**, 2096 (1970).
[7] B. Berglund, R. Tellegren, and J. O. Thomas, Acta Crystallogr. Sect. B **32**, 2444 (1976).
[8] B. Berglund and J. Tegenfeldt, Z. Naturforsch Teil A **32**, 134 (1977).
[9] B. Berglund and J. Tegenfeldt, J. Magn. Reson. **34**, 403 (1979).
[10] A. Sequeira, I. Bernal, I. D. Brown, and R. Faggani, Acta Crystallogr. Sect. B **31**, 1735 (1975).
[11] C. D. West, Z. Kristallogr. **88**, 198 (1934).
[12] G. Brink and M. Falk, Can. J. Chem. **49**, 347 (1971).
[13] (a) C. P. Slichter, *Principles of Magnetic Resonance* (Harper and Row, New York, 1963). (b) A. G. Redfield, Adv. Magn. Reson. **1**, 1 (1965).
[14] R. A. MacPhail, R. G. Snyder, and H. L. Strauss, J. Am. Chem. Soc. **102**, 3976 (1980), and work to be published.
[15] A. Chrétien, R. Kohlmuller, P. Pascal, and A.-P. Rollet, *Nouveau Traité de Chimie Minérale, Tome II, Premier Fascicule* (Masson et Cie, Paris, 1966), pp. 71, 76, and 346.
[16] E. Cornec and J. Dickeley, Bull. Soc. Chim. **41**, 1017 (1927).
[17] M. W. Routh, P. A. Swartz, and M. B. Denton, Anal. Chem. **49**, 1422 (1977).
[18] Curve Analysis Program supplied by Nicolet Instruments with the FTIR Spectrometer.
[19] W. H. Baur, Acta Crystallogr. **19**, 909 (1965).
[20] F. Bertaut, J. Phys. Radium **13**, 499 (1952).
[21] P. Ewald, Ann. Phys. **64**, 253 (1921).
[22] L. Fredin, B. Nelander, and G. Ribbegard, J. Chem. Phys. **66**, 4065 (1977).
[23] R. L. Somorjai and D. F. Hornig, J. Chem. Phys. **36**, 1980 (1962).
[24] (a) G. Baym, *Lectures on Quantum Mechanics* (Benjamin Cummings, Reading, Mass., 1969), p. 472; (b) The adiabatic approximation has also been used for similar systems by J. Wójcik and M. Falk [Chem. Phys. Lett. **56**, 450 (1978)], but the static limit instead of the limit of motional narrowing was chosen to determine the band shape. The static limit clearly does not apply to the systems discussed here.
[25] See, for example, G. Soda and T. Chiba, J. Chem. Phys. **50**, 439 (1969).
[26] This Fermi resonance has been observed in other hydrates, for example, $K_2CuCl_4 \cdot 2H_2O$ (Ref. 2, p. 92).
[27] Note that a correlated motion of the waters is required to trap the HDO; if the HDO molecules moved individually, the equivalence of the H and D positions [see Fig. 7(b)], would lead to only one band at low temperatures.
[28] We have assumed the standard two level optical Bloch equations. See Slichter [Ref. 13(a)] for further details.
[29] C. B. Harris, R. M. Shelby, and P. A. Cornelius, J. Chem. Phys. **70**, 34 (1979).
[30] D. W. Oxtoby, Annu. Rev. Phys. Chem. **32**, 77 (1981).